POLITECNICO MILANO 1863

SCUOLA DI INGEGNERIA INDUSTRIALE E DELL'INFORMAZIONE

Executive Summary of the Thesis

# Inclusion of reference wind turbine controller in wind tunnel experiments on the aerodynamic response of floating wind turbines

Laurea Magistrale in Mechanical Engineering - Ingegneria Meccanica

**Author:** Elio Daka

**Advisor:** Prof. Marco Belloli

**Co-advisor:** Ing. Alessandro Fontanella

**Academic year:** 2021-2022

---

## 1. Introduction

Wind energy has experienced an extraordinary growth in terms of installed capacity and wind turbines size. The commitments made globally during the cop26 to reach the net-zero scenario, will further drive wind energy growth, with floating offshore wind turbines (FOWT) being the main research target. With floating configuration regions with high wind speed quality can be exploited maximizing energy production.

In this framework the role of the wind turbine controller takes on an even more important role, because of the new challenges that arise with offshore turbines. The new generation of wind turbine controller have to deal with the peculiarities of the floating turbines, and should be easily adaptable to a large variety of cases.

The fast development of new design solutions and control ideas is made possible by the continuous improvement of dedicated numerical tools. Numerical simulations help to understand in advance possible critical issues that may occur in some particular operating condition of the wind turbine, without the need of a full-scale prototype.

Despite their incredible usefulness and accuracy, numerical software cannot predict all the possible behaviors of a wind turbine in real condition and experimental validations are needed. Wind tunnel tests on scaled prototypes are a costly-effective way to test a large number of different situations, helping to validate and improve numerical results. Also floating systems can be tested by mean of dedicated Hardware In the Loop (HIL) implementations.

## 2. ROSCO

The Reference Open Source COntroller (ROSCO) [1] provides a baseline controller, that addresses the issues of modern wind turbines, and can be easily adapted to a large variety of different models. The controller was firstly developed at Delft University of Technology and was designed to perform comparably to existing controllers already present in literature, and to be representative of the controllers used in industry. Furthermore, it was developed to have a simple tuning process, with the ambition that a control engineer is not needed to tune it for the specific wind turbine considered. Figure 1 shows the controller logic and block diagram.

The controller has a modular framework, with some modules dealing with the classical aspects

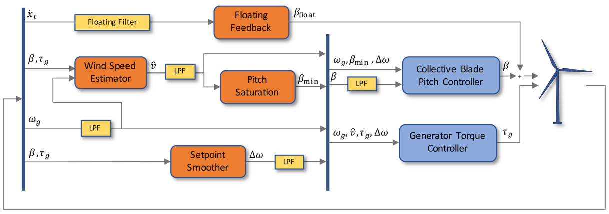


Figure 1: ROSCO controller logic [1].

of the control problem for wind turbines [2], and other dedicated to specific issues of floating systems. The foundation of the controller is a variable speed variable pitch controller. In below-rated region the blade pitch angle is kept fixed, while the generator torque is regulated with a PI controller in order to track an optimum rotor speed, guaranteeing maximum power extraction. In above-rated region, generator torque is kept constant and blade pitch regulated with a PI controller in order to keep the power extraction at the target level, limiting loads. Additional modules are present to address specific issues. Among these, the floating feedback module provides an additional control on the blade pitch angle to account for the oscillations of the platform, helping to stabilize the system.

## 3. IEA 15 MW RWT

The International Energy Agency 15 MW Reference Wind Turbine [3] has been developed by NREL and DTU, to serve as a reference for the new generation of floating wind turbines. The turbine is of Class IB with a rotor diameter of 240 m, and a hub height of 150 m. The turbine was developed for offshore applications with a monpile configuration, but a floating version has been developed by NREL and UMaine. Reference turbines serve as an open design benchmark that can be used to explore new solutions and, being publicly available, they allow the collaboration between industry and external researchers. Figure 2 shows the steady state operating points of the turbine.
The baseline controller proposed for the turbine is ROSCO, with TSR tracking in below rated region and constant torque in above rated. Numerical simulations in OpenFAST are performed to verify the controller behavior for wind speed steps. Figure 3 shows the simulation results. Despite the not negligible overshoot of rotor speed in correspondence of the wind step, the controller performances are good.

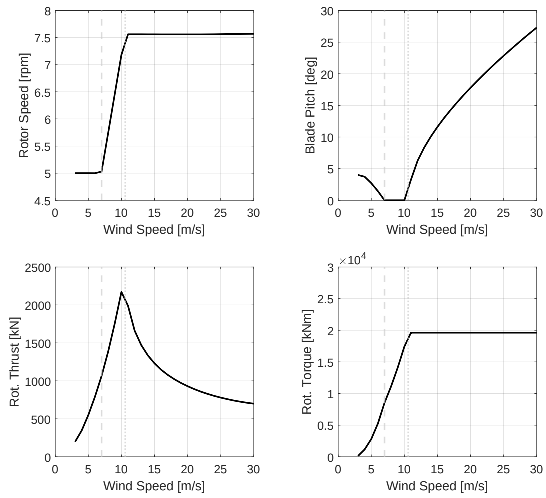


Figure 2: IEA 15 MW steady state points.

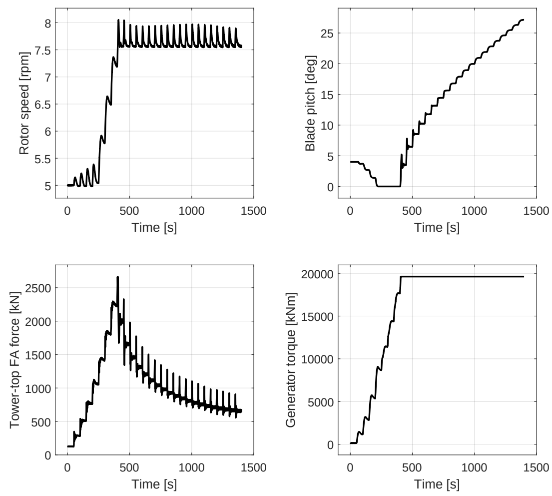


Figure 3: IEA 15 MW RWT response to wind speed steps.

## 4. POLIMI 15 MW WTM

The Polimi 15 MW Wind Turbine Model (WTM) is a 1:100 scaled prototype of the IEA 15 MW RWT. The model is designed to reproduce the performance of the reference turbine and to be suitable for wind tunnel tests.

### 4.1. Rotor Aerodynamic Design

In the design of scaled prototypes Froude and Reynolds similitude have to be taken into account. Froude similitude is important for floating structures, where the overall stiffness is mainly influenced by the weight of the structure, while Reynolds similitude is fundamental for aerodynamic forces. However, the two similitudes cannot be respected together. Besides, the dimensions and the flow speed of the wind tunnel add another contraint in the design process. The model was designed to exploit at the maximum the wind tunnel facility, leading to the scale factors reported in table 1.

| Scale factor | Definition | Value |
|---|---|---|
| Lenght | $n_{\mathrm{l}}$ | 100 |
| Velocity | $n_{\mathrm{v}}$ | 3 |
| Time | $n_{\mathrm{t}} = n_{\mathrm{l}}/n_{\mathrm{v}}$ | 100/3 |
| Frequency | $n_{\omega} = n_{\mathrm{v}}/n_{\mathrm{l}}$ | 3/100 |
| Mass | $n_{\mathrm{m}} = n_{\mathrm{l}}^3$ | $100^3$ |
| Force | $n_{\mathrm{F}} = n_{\mathrm{l}} n_{\mathrm{m}}/n_{\mathrm{t}}^2$ | $100^3$ |

Table 1: Scale factors for the PoliMi 15 MW turbine model.

With these scale factors the Reynold similitude is not respected, so a specific procedure described in [4] is followed to design the turbine blades. According to this design methodology, the prototype lift distribution along the blade span matches the one of the full-scale model. To ensure this, low Reynolds airfoils were used, and chord length distribution and blade twist were optimized. Given that the drag coefficient is not fully controlled in the design procedure, some discrepancies in the $C_p$ curve are expected and accepted.

## 4.2. Numerical Model

In order to simulate the response of the Polimi 15 MW WTM, a numerical model for OpenFAST v3.1.0 [5] was developed. ROSCO was tuned for the numerical model and simulation was performed to verify the behavior of the system and to check the goodness of the controller. The numerical model was implemented up-scaling the prototype to the full-scale size, in order to have a direct comparison with the results obtained for the IEA 15 MW RWT. The model is considered rigid and only the rotor degree of freedom is active.
The ROSCO controller was tuned following the procedure indicated in [1], modelling the system a single degree of freedom system:

$$J^* \dot{\omega}_g = N_{gb}(\tau_a - N_{gb}\tau_g\eta_{gb}) \tag{1}$$

where $J^*$ is the equivalent inertia at rotor side, $N_{gb}$ is the gearbox reduction ratio, $\eta_{gb}$ is the gearbox efficiency, $\tau_g$ is the generator torque, and $\tau_a$ is the rotor aerodynamic torque. After linearization and the introduction of the torque sensitivities the equation can be written as:

$$\Delta\dot{\omega}_g = \frac{1}{J^*}K_{\omega Q}\Delta\omega_g + \frac{N_{gb}}{J^*}K_{\beta Q}\Delta\beta + \\ + \frac{N_{gb}}{J^*}K_{UQ}\Delta U - \frac{N_{gb}^2}{J^*}\eta_{gb}\Delta\tau_g \tag{2}$$

where $K_{\omega Q}, K_{\beta Q}, K_{UQ}$ are the aerodynamic torque sensitivities with respect to rotor speed, blade pitch angle and wind speed respectively, that are function of the operating point. Equation 2 is the starting point for the tuning procedure. Figure 4 shows the steady state points obtained through the numerical model compared to the one of the reference wind turbine.

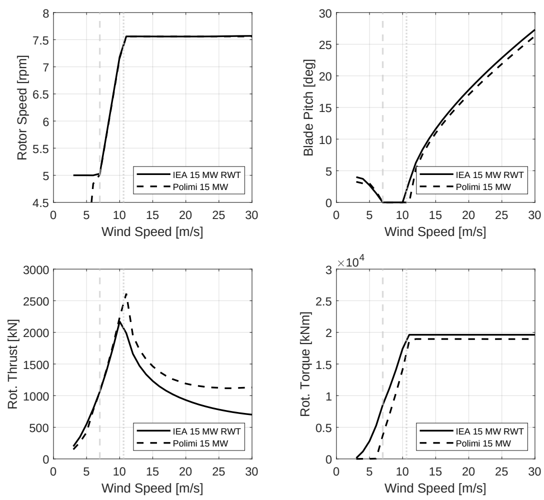


Figure 4: Steady state operating points of the Polimi 15 MW compared to the ones of the IEA 15 MW RWT. The grey dashed and dotted line represents the transition regions.

To verify the controller behavior, the system has been simulated subjected to laminar wind speed steps, from 3 m/s to 30 m/s. Figure 5 shows the results obtained through OpenFAST simulations. The controller performances are good compared to the ones of the reference turbine presented in figure 3. Differences can be noted for rotor speed and generator torque mainly. Discrepancies in the equivalent inertia and the aerodynamic sensitivities between the Polimi 15 MW WTM and the IEA 15 MW WTM, lead to different system dynamics and controller parameters. At the end, this causes differences in the controller performances. In particular, the Polimi 15 MW WTM has an higher rotor inertia, causing lower rotor speed overshoot and higher generator torque undershoot in correspondence of the wind step.

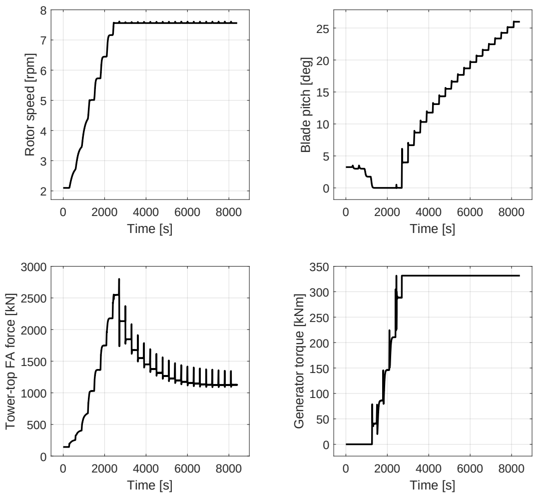


Figure 5: System response to wind speed steps.

# 5. Wind Tunnel Tests

The wind turbine model was deployed in the 'Politecnico di Milano Wind Tunnel' mounted on an hexapod, that can reproduce the off-shore condition through a numerical model. Two set of tests were performed: static and imposed motion.

## 5.1. Static Tests

In static tests the goal was to verify the steady state operating points of the model, compared to the numerical model and to the reference turbine.

Steady state values of thrust and torque at different wind speed are important to understand the static loads that the turbine undergoes during its life. Moreover, static values of blade pitch and rotor speed, are important to characterize the wake of the turbine downwind, to investigate the reciprocal position of the turbines in a wind farm.

Three wind speeds in the above-rated region and one in the below-rated region, but near the rated speed, were considered. Testing the below-rated region is difficult because of the very low scaled velocities of the wind tunnel flow. At this low speeds the limited Reynolds number causes a drop in the aerodynamic efficiency of the blades, and the rotor cannot generate torque or power.

Experimental results, in terms of mean value over 60 seconds of acquisition, are presented in figure 6, reported on the steady state operating points of the Polimi 15 MW numerical model and of the IEA 15 MW RWT.

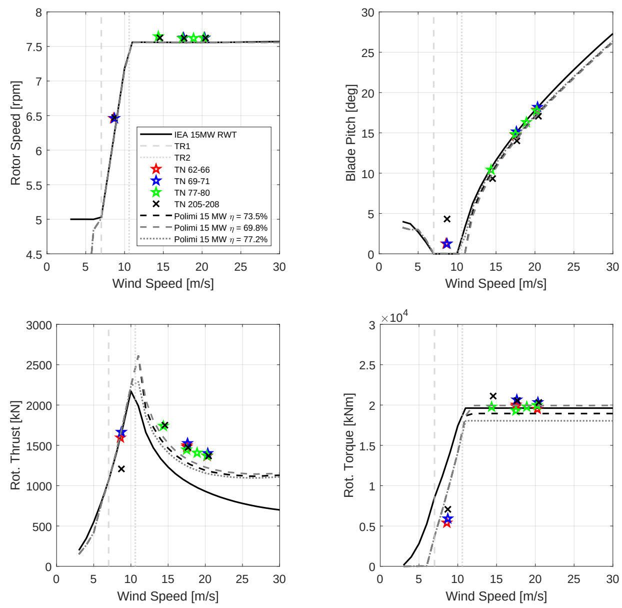


Figure 6: Experimental results of static tests, upscaled and reported on the steady state curves of the IEA 15 MW RWT and of the numerical model of the Polimi 15 MW.

Discrepancies can mainly be attributed to sensor systematic errors and wrong parameter estimation. The main parameter affecting the results is the gearbox efficiency, that affects the generator torque and consequently the blade pitch angle and thrust. Steady state points obtained from the numerical model at different gearbox efficiency, suggests that this parameter was overestimated by at least 5%.

Overall, the results are promising, with a good agreement between experimental and numerical results. The model reproduces good enough the steady state values of the IEA 15 MW RWT in above-rated condition. In below-rated region the results are quite different in terms of torque, mainly due to the Reynolds effect, but this aspect is correctly reproduced by the numerical model.

## 5.2. Imposed Motion Tests

During imposed motion tests, a sinusoidal motion in pitch direction have been imposed to the hexapod, in order to verify the behavior of the

controller in an off-shore configuration.
The sinusoidal motion of the platform causes an apparent wind speed at the rotor that acts as a disturbance, to which the controller reacts. The response of the system to this action depends on the undisturbed wind speed, the system physical properties (such as rotor inertia), the aerodynamic sensitivities and the controller gains. In order to reproduce in the experiment what is obtained through the numerical model, all the involved quantities should be properly scaled according to the scale factors presented in table 1. The correct scaling is ensured for the controller gains and the rotor inertia. Aerodynamic sensitivities of the rotor with respect to rotor speed, blade pitch and wind speed are formulated as:

$$
\begin{aligned}
K_{\omega Q} &= \frac{\tau_{a,0}}{\omega_{g,0}} \left( \left. \frac{\partial C_Q}{\partial \lambda} \right|_0 \frac{\lambda_0}{C_{Q,0}} \right) \\
K_{\beta Q} &= \frac{1}{2} \rho \pi R^3 U_0^2 \left( \left. \frac{\partial C_Q}{\partial \beta} \right|_0 \right) \qquad (3) \\
K_{UQ} &= \frac{\tau_{a,0}}{\omega_{g,0}} \left( 2 - \left. \frac{\partial C_Q}{\partial \lambda} \right|_0 \frac{\lambda_0}{C_{Q,0}} \right)
\end{aligned}
$$

These values depend on the steady state operating point of the rotor and on the torque nondimensional coefficient $C_Q$, that is characteristic of the rotor itself. Effort has been spent in simulating the same operating points obtained during wind tunnel tests, but the discrepancies in torque coefficient cannot be mitigated, thus some discrepancies will be accepted. Results are presented after filtering and time-averaging, focusing on the frequency component equal to the motion frequency.
Figure 7 shows the results for the imposed motion at frequency f = 1.25 Hz in below-rated region. Thrust, torque, rotor speed and blade pitch are reported.
The matching between experimental and numerical results is quite good for thrust force, while it is not for rotor torque and rotor speed. In particular, amplitudes of oscillations are higher in the numerical test for rotor torque, and smaller for rotor speed. The different phase observed in rotor speed causes the phase shift in the rotor torque. The difference in rotor torque oscillation can be attributed to the different blade pitch angle. Indeed, during the tests was not possible to precisely set the zero blade pitch angle position. This can also explain the lower torque mean value, in agreement with the results presented for static tests.

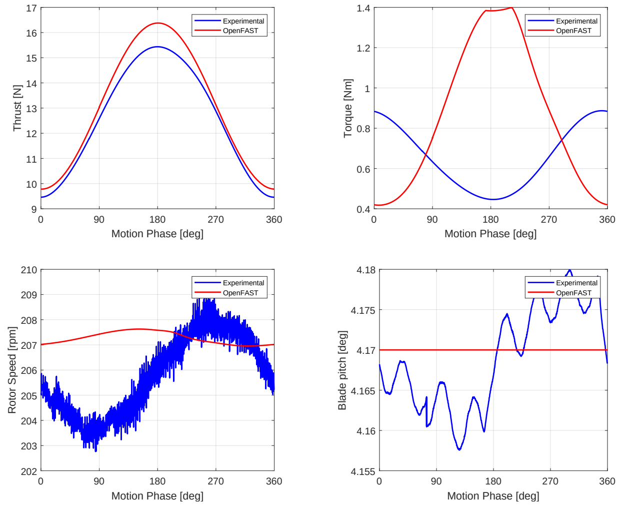


Figure 7: Comparison between experimental and numerical results for imposed motion test at f = 1.25 Hz, in below-rated region.

Figure 8 shows the results for the same test in above-rated region.

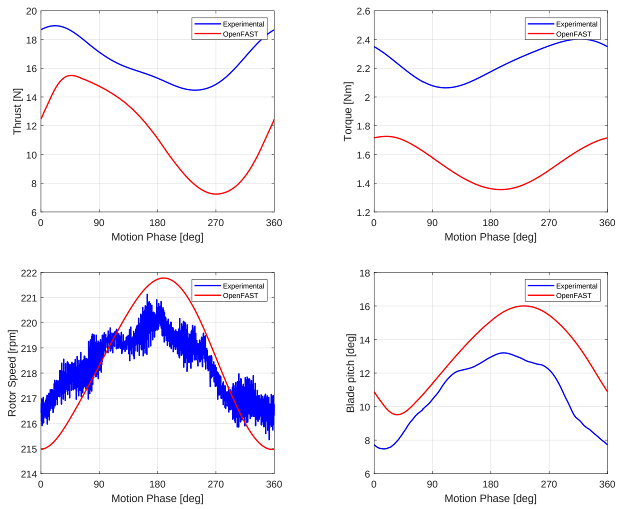


Figure 8: Comparison between experimental and numerical results for imposed motion test at f = 1.25 Hz, in above-rated region.

In above-rated region, thrust and rotor signal are similar in oscillation amplitudes, but the mean value and the phase present not negligible differences. Differences in mean value can be explained by the different mean value of blade pitch, which can be attributed to two factors. First, a not precise setting of the zero pitch an-

gle, and second to a wrong estimation of drive-train efficiency. Indeed, a lower real efficiency brings a higher torque at rotor side, and consequently to a lower blade pitch angle. It should also be mentioned that the acquired blade pitch signal is the reference blade pitch coming from the controller. This signal passes through the transfer function of the pitch actuator that modifies the signal, adding another source of uncertainty. This effect is compensated in the post-processing of data, but some errors can still be present.
In above-rated test, discrepancies in phase are less evident. This is because the better matching of rotor speed phase and blade pitch angle phase between experimental and numerical results.

## 6. Conclusions

A numerical model for the Polimi 15 MW WTM has been developed. More attention has been paid on the wind turbine controller, in particular the ROSCO controller was tuned for the model. The response of the numerical model under different wind speed conditions was verified through OpenFAST simulations, comparing the results with the ones of the IEA 15 MW RWT. An overall good matching between the two models was observed, both for steady state points and controller dynamic performances. The controller was implemented in Simulink® allowing to implement the controller on the prototype and perform wind tunnel tests.
Results for static tests are satisfying, with a good matching between experimental and numerical results. Discrepancies are mainly due to the errors in parameter estimation, like the gearbox and generator efficiency, and to the Reynolds effect of the rotor.
For imposed motion tests results are promising, but there are more discrepancies between experimental and numerical results. Some of them can be related to the experimental set-up, which can be perfected, but others requires further studies. The tuned and implemented controller allows to experimentally test the dynamic performance of the controller. It also makes it possible to fully exploit the exapod in a Hardware-In-the-Loop configuration, verifying the response of the system and of the controller in off-shore configurations.

## References

[1] Nikhar J. Abbas, Daniel S. Zalkind, Lucy Pao, and Alan Wright. *A reference open-source controller for fixed and floating offshore wind turbines.* *Wind Energy Science*, 7(1):53–73, 2022.

[2] Bianchi Fernando D., Hernan. De Battista, and Ricardo J. Mantz. *Wind Turbine Control Systems Principles,Modelling and Gain Scheduling Design.* Springer, London, 2011.

[3] Evan Gaertner et al. *IEA Wind - Offshore Reference Wind - 15MW.* Technical report, National Renewable Energy Laboratory, 2020.

[4] Ilmas Bayati, Marco Belloli, Luca Bernini, and Alberto Zasso. *Aerodynamic design methodology for wind tunnel tests of wind turbine rotors.* *Journal of Wind Engineering and Industrial Aerodynamics*, 167:217–227, 2017.

[5] National Renewable Energy Laboratory. *OpenFAST Documentation*, 2022. URL `https://openfast.readthedocs.io`.